J Solid State Electrochem (2010) 14:175–184
DOI 10.1007/s10008-009-0879-1

ORIGINAL PAPER

A rotating disc electrode study of oxygen reduction at platinised nickel and cobalt coatings

Andromahi Tegou · Sofia Papadimitriou · Georgios Kokkinidis · Sotirios Sotiropoulos

Received: 30 December 2008 / Revised: 16 April 2009 / Accepted: 2 June 2009 / Published online: 23 June 2009

Abstract Platinized nickel and cobalt coatings, Pt(Ni) and Pt(Co), have been prepared on glassy carbon, GC, rotating disc electrode substrates by a two-step room temperature procedure that involved the electrodeposition of nickel and cobalt layers and their spontaneous partial replacement by platinum ("transmetalation") when immersed into a chloroplatinic acid solution. By tuning the quantity of initially deposited nickel and cobalt, Pt(Ni) and Pt(Co) bimetallic coatings having a 26% atom Ni and 30% atom Co composition have been prepared. For both materials typical Pt surface electrochemistry was recorded during fast voltammetry in deaerated acid, pointing to the existence of a continuous Pt skin over a Pt–Ni and Pt–Co core. Oxygen reduction at the Pt(Ni)/GC and Pt(Co)/GC electrodes was studied by means of steady-state voltammetry at a rotating disc electrode and the construction of Tafel plots from corresponding voltammetric data. It was found that, when the initial potential of the voltammetric sweep allowed the formation of a complete Pt oxide monolayer, then oxygen reduction was hindered for low overpotentials at Pt(Ni) and Pt(Co), compared to pure bulk Pt. On the other hand, when the initial potential was less positive (thus leading to the formation of a fraction of surface oxide monolayer) the presence of Ni and Co enhanced the kinetics of oxygen reduction. The former behaviour is attributed to a decrease in oxide reduction ability of Pt in the presence of Ni and Co, while the latter to an increase in dissociative oxygen chemisorption due to Ni and Co.

Keywords Platinum catalysts · Bimetallic catalysts · Oxygen reduction · Transmetalation

Introduction

Bimetallic Pt–Ni and Pt–Co catalysts have been extensively studied as improved cathodes for the oxygen reduction reaction (ORR) both in carbon-supported forms (see for example [1–13]) and as films or bulk alloys [4, 14–22]. The beneficial effect of the early-transition metals on Pt could either be due to changes in the Pt–Pt distance that favour dissociative oxygen chemisorption, or to the formation of surface oxides on the second metal instead of Pt (where they would inhibit ORR) [3, 4, 23–25], or to an electronic effect (attributed either to an increase of the Pt d-vacancy character) [1, 2, 6, 12, 15, 24–28] or to a d-band energy level, ε_d, lowering [17–20, 22]. Depending on the preparation of the catalysts and their resulting surface composition the contribution of the above effects may vary. If Ni and Co are exposed to the reaction medium then the first two effects are expected to be dominant. If, however a Pt skin is formed around the catalyst particles (either due to annealing-induced segregation [29] during preparation or transition metal leaching during electrode operation in an acid medium [2, 3, 13–20]), then only the electronic effect of the underlayers can be operative.

The preparation of platinum-based alloy or bimetallic catalysts is usually carried by impregnation of high-surface-area carbons with the metal ions which are then reduced either by high temperature hydrogen treatment [1–4] or by a room temperature reducing agent in solution phase (such as

Electronic supplementary material The online version of this article (doi:10.1007/s10008-009-0879-1) contains supplementary material, which is available to authorized users.

A. Tegou · S. Papadimitriou · G. Kokkinidis · S. Sotiropoulos (✉)
Department of Chemistry, Aristotle University of Thessaloniki, Thessaloniki 54124, Greece
e-mail: eczss@chem.auth.gr

borohydride, glycols, formic acid etc.) [5–9, 11, 12]; in the microemulsion method variant of the room temperature techniques the metal particles are formed first (by mixing the metal salt and reducing agent microemulsions) and then adsorbed onto the carbon powder support (see for example [10]). Well-defined films of these catalytic materials prepared for fundamental studies can be produced by metallurgical [4, 16] or sputtering processes [14, 15].

During the last decade an alternative room temperature method has been proposed for the preparation of bimetallic (and multi-metallic) catalyst materials. The method (termed as "transmetalation") is based on the spontaneous replacement reaction of surface layers of a non-noble metal (e.g. Cu, Pb, Co, Ni etc.) by a noble metal (e.g. Pt, Au, Pd etc.) when particles or layers of the first metal are immersed into a solution of the noble metal complex ions. Two variants of the technique have been established. In the first one, introduced and followed by Adzic and co-workers (see for example [30–38]), a Cu UPD monolayer that has been electrodeposited on a precious metal substrate (e.g. Pd, Au, Ru or Pt), is fully replaced by one or more of other noble metals (e.g. Au, Pt, Pd, Ir, Ru, Rh, Re, Os), resulting in noble–noble metal interactions in the outer catalyst layers and significant decrease in the second noble metal loading. In the other one, introduced by Kokkinidis and co-workers [39, 40] and further developed by Sotiropoulos and co-workers [41–44], the substrate consists of electrodeposited non-noble metal multilayers (e.g. Pb, Cu, Fe, Co, Ni) and its surface layers are replaced by the noble metal (e.g. Pt, Au). The latter catalysts are characterised by noble–non-noble metal interactions in the outer layers. In our previous studies of ORR at platinized Pb, Cu, Fe, Co and Ni layers (Pt(M), with M being the substrate metal) we found that although the catalytic activity of Pt(Pb) and Pt(Cu) electrodes was similar or better than that of pure Pt (at low or high overpotentials respectively), that of Pt(Fe), Pt(Co) and Pt (Ni) was inferior at all polarizations [42, 44]. These results were unexpected since there is extensive experimental and theoretical literature pointing to enhancement of ORR (to various extents) at Pt–Co and Pt–Ni electrodes [1–28]. This has prompted us to critically review those results and investigate the possible reasons of the observed different behaviour. There are at least three differences in the experimental conditions between our studies and those in the literature. First, our Pt(Ni) and Pt(Co) catalysts had a low Ni and Co content, less than the 25% atom concentration typical of the Pt_3Ni and Pt_3Co formulations mainly studied. Second, the initial potential of the voltammetric scans we used to access the ORR activity was more positive (+1.20 V vs. Ag/AgCl (3 M NaCl) in 0.1 M $HClO_4$) than the rest potential of the system (ca. +0.85 V) and the majority of initial potential values used in the literature (in the +0.75–+0.85 V vs. SCE range in 0.1 M $HClO_4$). Finally, unlike our catalysts, in many of the studies of the kind the degree of alloying had been improved by a final annealing step. In view of the above, we thought it was worth revisiting the performance of the Pt(Ni) and Pt(Co) layers prepared by transmetalation, under composition and voltammetric conditions closer to those of the relevant literature.

The aim of this work has therefore been to study the effects of (a) an increased Ni and Co atomic percentage composition of the Pt(Ni) and Pt(Co) deposits and (b) a decreased anodic limit of steady-state voltammetry on the ORR electrocatalytic activity of these electrodes. Specific objectives have been: (1) to tune the composition of the Pt (M) systems by varying the quantity of initial M deposited, (2) the comparison of ORR voltammetric data from acid solutions, obtained at Pt(M) layers deposited on a glassy carbon (GC) rotating disc electrode (RDE) with two different initial anodic potential limits and (3) the identification of optimum preparation and appropriate evaluation conditions for improved Pt(Ni) and Pt(Co) ORR catalysts prepared by the transmetalation method.

Experimental

Preparation of Pt(Ni)/GC and Pt(Co)/GC electrodes

Electrodeposition of Ni on GC disc electrodes (5 mm diameter) was carried out from 0.01 M Ni sulfamate + 0.227 mM $NiCl_2$ + 0.025 M H_3BO_3 deaerated solutions at −1.1 V vs. SCE. The plating current efficiency was found to be 97–99%. The charge density passed was varied in the 157–787 mC cm^{-2} range, producing the equivalent of 300–1,500 flat Ni monolayers (assuming a 98% current efficiency, a FCC crystal structure and a 0.1246 nm atomic radius [45] for Ni). Co was electrodeposited from 5 mM $CoCl_2 \cdot 6H_20$ + 0.1 M $MgSO_4 \cdot 7H_20$ + 0.1 M H_3BO_3 deaerated solutions at −1.00 V vs. SCE with current efficiency in the 93–97% range. The total charge density was varied between 176 and 878 mC cm^{-2}, resulting to the equivalent of 300–1,500 flat Co monolayers (assuming a 95% current efficiency, an equimolar mixture of HCP and FCC crystal structures, and a 0.1253 nm atomic radius [45] for Co). Taking into account the density of bulk Ni and Co metals [45], the thickness of the coatings is estimated to have been varied in the 54–268 nm range for Ni and 61–303 nm for Co. The Ni/GC and Co/GC electrodes were then immersed in a 0.1 M HCl + 10−3 M K_2PtCl_6 solution for 30 min so that spontaneous Ni and Co replacement by Pt occurred:

$$2\,\mathrm{Ni/GC} + \mathrm{PtCl_6^{2-}} \rightarrow \mathrm{Pt(Ni)/GC} + 2\mathrm{Ni^{2+}} + 6\mathrm{Cl^-} \quad (1)$$

$$2\,\mathrm{Co/GC} + \mathrm{PtCl_6^{2-}} \rightarrow \mathrm{Pt(Co)/GC} + 2\mathrm{Co^{2+}} + 6\mathrm{Cl^-} \quad (2)$$

Microscopic and spectroscopic characterisation of coatings

Scanning electron microscopy (SEM) was carried out using a JEOL JSM-5510 microscope and elemental analysis of the coatings was performed by the accompanying EDS (EDAX) system.

Electrochemical characterisation of coatings

Potentiostatic deposition and voltammetry was carried out using the Autolab 100 (EcoChimie) system, in small three-compartment cells equipped with a luggin capillary at the end of the reference electrode (Saturated Calomel Electrode, SCE, Radiometer) chamber. The counter electrode was a Pt coil. Experiments were carried out in three different cells to ensure minimum contamination. In the first one the core Ni or Co metal elecrodeposition was carried out. In the second cell the Pt(Ni)/GC and Pt(Co)/GC electrodes were activated-etched by repetitive potential cycling at 1 V s^{-1} in 0.1 M $HClO_4$ solution between hydrogen and oxygen evolution (i.e. between −0.35 and +1.25 V vs. SCE) with any particles containing uncovered Ni and Co dissolving away during potential excursion to anodic values. In the third cell Pt surface electrochemistry and oxygen reduction at the fully Pt-covered Pt(Ni) and Pt (Co) layers were studied in clean acid solutions.

Electrode materials and chemicals

The electrode substrate consisted of a glassy carbon (3 mm diameter) RDE controlled by a Taccusel EDI101T motor. After each set of experiments, the electrode was treated for 30 s with aqua regia to ensure complete etching of the Pt(Ni) and Pt(Co) deposits and then polished on emery paper and finally on alumina powder of 0.1 and 0.01 μm particle size (Buehler). The pure Pt (2 mm diameter) RDE employed in comparative experiments was fabricated from metal rods (Goodfellow; 99.95%). The electrode substrates used for SEM/EDS characterization were fabricated from glassy carbon 1-mm thick plates (Alfa Aesar) that were cut into 3-mm diameter discs. They were sealed to a glass tube body with a shrinkable thermoplastic tube and electrical contact between the disc and a commercial wire inserted from the open end of the glass tube was achieved with mercury.

HClO4 from Riedel, (puriss p.a., ACS reagent, ≥70%) was employed in the preparation of electrodeposition solutions and in ORR experiments. $CoCl_2 \cdot 6H_2O$ and $MgSO_4 \cdot 7H_20$ from Merck (p.a. 99%) and H_3BO_3 (puriss 98%) from Aldrich were used for the preparation of the Co deposition solutions and Ni sulfamate (p.a. 99%) from Fluka, $NiCl_2$ (puriss >97%) from Merck and H_3BO_3 (puriss 98%) from Aldrich for Ni deposition solutions. H_2PtCl_6 hexahydrate from Sigma-Aldrich (ACS reagent, ≥37.50% as Pt) was used for the preparation of the Pt exchange solution.

Results and discussion

SEM/EDS characterisation of Pt(Ni) and Pt(Co) deposits

Figure 1a, c show SEM micrographs of the electrodeposited Ni and Co layers (equivalent of 300 flat monolayers, 300 eq-ML) on the GC substrate. Relatively smooth deposits can be seen, similar to those corresponding to thicker layers (1,000–1,500 eq-ML) presented in [43, 44]. Figure 1b, d show the corresponding micrographs after immersion of the above samples into chloroplatinic acid for 30 min and subsequent treatment of the resulting Pt(Ni)/GC and Pt(Co)/GC electrodes in perchloric acid by potential cycling between hydrogen and oxygen evolution. As a result of uneven deposit transmetalation and subsequent electrochemical etching of unreacted particles, the platinized and electrochemically treated layers exhibit now a more roughened texture. They still consist however of continuous and relatively smooth films when compared to their analogues prepared by thicker initial deposits [43, 44]. Supplementary grazing incidence XRD measurements allowed the estimation of Pt crystallite size in the 9–12 nm range. To study the effect of deposit thickness on the final composition of the catalytic layers, a detailed EDS analysis of coatings produced from the transmetalation of initial electrodeposits of varied thickness was carried out. Its results are presented in Table 1 from which it follows that the relative percentage of Ni and Co increases as the thickness of the original electrodeposits decreases.

Both the composition and morphology trends with deposit thickness variation can be rationalised as follows. The transmetalation process is a surface exchange reaction (etching of the non-noble metal by the depositing noble metal) and is terminated when all Ni and Co surface locations are either covered by Pt or inaccessible to the exchange solution (e.g. by being deep inside a porous film). At the same time, it is not expected to occur either at the same rate at all locations or by the formation of an ideal Pt monolayer; for example, Pt atoms may deposit on already deposited Pt nuclei while Ni and Co are further etched from nearby locations, resulting in an etched three-dimensional network. This means that Pt and Ni (or Co) are well-mixed even inside the core of the resulting layers, as has been experimentally verified by sputter-etch Auger electron spectroscopy for Pb and Cu [43, 44]. As thicker deposits undergo the tansmetallation process this is prolonged since the deposit can be etched deep inside the initial layer, supporting more Pt deposition at surface locations and thus increasing the Pt-to-non-noble metal ratio. Also, the

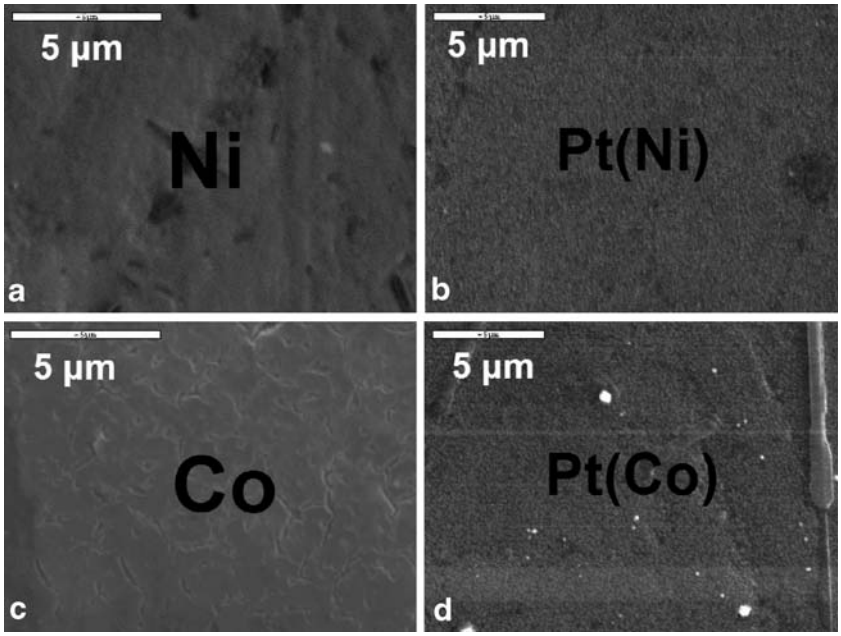

Fig. 1 SEM micrographs of: **a** a 300 eq-ML thick Ni electrodeposit on a GC electrode; **b** the resulting Pt(Ni) coating prepared by 30 min immersion of (**a**) in a 0.1 M HCl+10−3 M K_2PtCl_6 solution, followed by electrochemical treatment between hydrogen and oxygen evolution potentials; **c** a 300 eq-ML thick Co electrodeposit on a GC electrode; **d** the resulting Pt(Co) coating prepared from (**c**) by a procedure identical to that followed for (**b**)

existence of a three-dimensional porous structure within the deposit may give rise to unreacted non-noble metal areas, shielded from Pt due to mass transfer limitations but prone to anodic dissolution during electrochemical treatment, thus leading to further increase of the above-mentioned ratio as well as to sparser deposits. Note, that similar behaviour, namely prolongation of the transmetalation process and incomplete non-noble metal protection (as inferred by persisting high anodic currents despite multiple potential scans), was observed in attempts to platinize pure compact Ni and Co disc electrodes. On the contrary, at thin Ni and Co films the deposit is quickly etched at locations down to the substrate and the rest of the metal is rapidly protected by thin Pt layers. This would explain both the higher non-noble metal content and the continuity of the resulting Pt(Ni) and Pt(Co) films prepared from thinner initial deposits.

It is important to note that, whatever the origin of these initial electrodeposit thickness effects may be, they allow the control of catalyst composition to levels comparable with those of bimetallic catalysts prepared by other techniques (i.e. in the 20–30% Ni and Co atomic percentage range).

Table 1 Relative atomic percentage composition of Pt(Ni) and Pt(Co) deposits as obtained from EDS analysis

Number of initially electrodeposited Ni or Co monolayers	Atomic percentage composition of Pt(Ni) and Pt(Co) deposits in Pt, Ni or Co/%			
	Pt(Ni)		Pt(Co)	
	Pt	Ni	Pt	Co
300	74	26	70	30
600	81	19	78	22
1,000	84	16	93	7
1,500	92	8	98	2

Samples were prepared by the transmetalation of electrodeposits of varied initial thickness (expressed as the number of initially deposited equivalent flat monolayers of Ni or Co)

Surface electrochemistry of Pt(Ni)/GC and Pt(Co)/GC electrodes in acid

Figure 2 presents potential sweep voltammograms for Pt(Ni)/GC and Pt(Co)/GC electrodes in clean deaerated 0.1 M $HClO_4$ solutions, after having been cleaned by potential cycling in a separate solution (see "Experimental"). Figure 2a, b correspond to situations where the anodic potential limit was +1.20 V vs. SCE (i.e. just prior to oxygen evolution and corresponding to the formation of a complete Pt oxide monolayer) and +0.90 V (corresponding to the formation of a partial Pt oxide monolayer). The voltammetric picture obtained is similar to that of bulk Pt and typical of polycrystalline Pt surface electrochemistry (characterised by hydrogen adsorption/desorption peaks and oxide formation/stripping wave/peak), indicating full surface platinization of the catalyst. The slight asymmetry between the cathodic and anodic H adsorption/desorption conjugate peaks is not likely to be due to the re-deposition

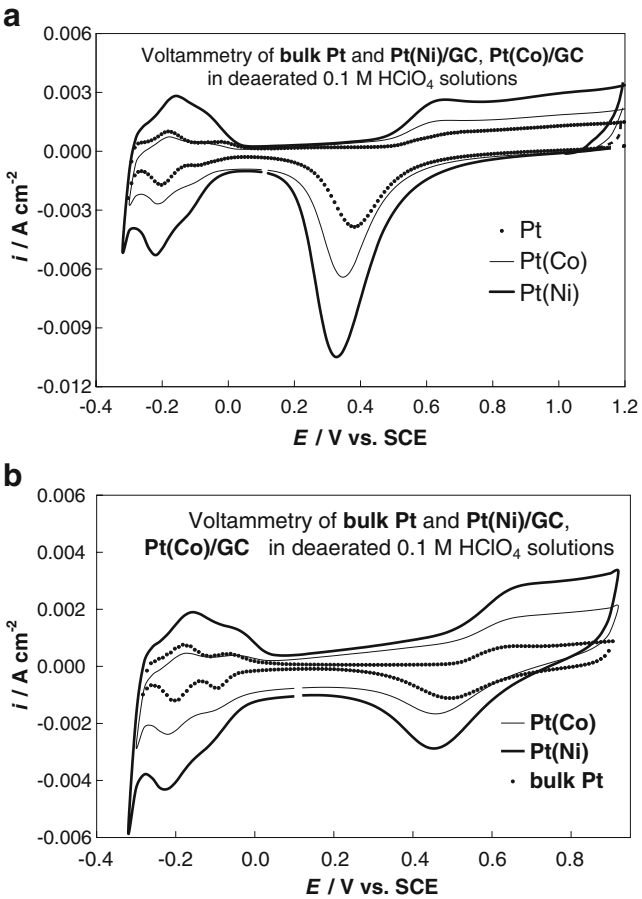

Fig. 2 **a** Cyclic voltammograms of Pt(Ni), Pt(Co) and Pt electrodes in a deaerated 0.1 M $HClO_4$ solution with a +1.20 V vs. SCE positive potential limit (at a scan rate of 1 V s^{-1}). **b** Same as in (**a**) but with a +0.90 V vs. SCE positive potential limit

of Ni or Co ions (produced by the dissolution of uncovered surface quantities of these metals during the excursion of the potential to positive values). First of all, as already stated in the "Electrochemical characterisation of coatings", before the recording of the voltammograms of Fig. 2, the electrodes had been repeatedly scanned into the oxygen evolution potential range in a separate cell, so that any uncovered/unprotected surface Ni and Co was removed by transpassive dissolution. Second, the voltammetry presented here was stable in time, opposite to what it would be expected if parts of the deposit were continuously dissolving away due to Ni or Co dissolution at locations; that would lead to gradual Pt(Ni) and Pt(Co) disintegration and would be reflected in a changing voltammetric picture. Hence, the origin of the observed asymmetry has to be traced elsewhere. We believe that it is due to ohmic distortion of the high currents observed at the relatively high potential sweep rates (1 V s^{-1}) used to improve the accuracy of H adsorption/desorption charge estimation (see below). It has been found (both in this and our previous work [42]) that this asymmetry is removed at lower sweep rates. In all cases, however, the trends observed for the Pt oxide stripping peaks remained unchanged.

An estimate of Pt electroactive surface area, A_{esa}, was made by calculating the charge associated with hydrogen adsorption and assuming that 210 μC cm^{-2} correspond to the formation of a H monolayer [46]. The ratio $r=A_{esa}/A_{sga}$, where A_{sga} is the substrate geometric area, can be used for the quantification of Pt electroactive surface area and was found r=3.41, 1.31 and 1.10 for the Pt(Ni)/GC, Pt(Co)/GC and bulk Pt electrodes of Fig. 2. The small electroactive areas are in line with the continuous deposits depicted in the SEM micrographs of Fig. 1. The higher roughness factor of the Pt(Ni) deposits, although within the experimental variation of r factors calculated for this type of deposits [43], may be ascribed to finer Pt(Ni) particles as inferred from Fig. 1b, d.

A significant feature of Fig. 2a, b is the shift of the Pt oxide cathodic stripping peak to more negative potentials as one passes from pure Pt to Pt(Ni) and Pt(Co) (a trend present irrespective of the scan rate used), since the position of the Pt oxide cathodic may provide macroscopic evidence for the modification of the Pt–O bond strength or/and the rate of Pt surface oxide reduction due to the presence of the second metal. Depending on whether the initial potential was +1.20 or +0.90 V vs. SCE, this cathodic shift was –40 mV and –30 mV, respectively. Note that we observed similar cathodic shifts (indicating a retardation of surface oxide reduction) for Pt(Co) and Pt(Ni) catalysts prepared by thicker initial deposits (as well as for Pt(Cu), Pt(Fe) and Pt(Pb) catalysts) and for various potential scan rates in the 100–1,000 mV s^{-1} range [41–44]. This finding is in contrast with some findings and the overall views of Ross, Markovic, Stamenkovic and co-workers [3, 4, 16–20] who show some voltammetric evidence for difficult surface oxide formation and facile stripping at Pt_3Ni and Pt_3Co electrodes prepared and/or treated at high temperatures. They use these results to support the claim for a lower coverage by Pt surface oxides, in line with the theoretical predictions for a weakening of Pt–O and Pt–OH bond strength [47], which is in turn based on the more general DFT theory of Nørskov and co-workers [48, 49] that predicts a Pt d-band centre (ε_d) down-shift in the presence of early-transition metal underlayers. However, a careful inspection of the surface voltammetry of Pt–M (where M: Fe, Co, Ni) electrodes that appear in the relevant literature reveals the following. A clear shift of the Pt oxide stripping peak to more positive potentials is indeed presented by Stamenkovic et al. for Pt_3Fe in [19] and for $Pt_3Ni(111)$ in [20] as well as for carbon-supported Pt_3Ni and Pt_3Co by Paulus et al. in [3, 4]. However, no clear shift can be observed in some of the above references for $Pt_3Ni(100)$ and $Pt_3Ni(110)$ [20] as well as for unsupported Pt_3Ni and

Pt_3Co [4]. Furthermore, there are voltammetric data in the literature that point to an opposite shift of the oxide reduction peak (i.e. to more negative potentials, as our results suggest), namely for Pt_3Fe [15] and Pt_xCo_y electrodes [21].

Summarising, our results suggest that, at Pt(Ni) and Pt (Co) electrodes prepared by the room temperature transmetalation method, the reduction of Pt surface oxides (corresponding to both a complete and a partial oxide monolayer) is hindered when compared to pure Pt, indicating a higher coverage of oxygenated species. Note that Watanabe and co-workers has recently provided direct experimental evidence (using X-ray photoelectron spectroscopy (XPS)) that the surface of $Pt_{63}Fe_{37}$ electrodes has a similar coverage of OH_{ads} and a higher coverage of O_{ads} species than pure Pt [22].

Oxygen reduction reaction in acid at Pt(Ni)/GC and Pt(Co)/GC RDEs

Figure 3a, b show voltammograms for Pt(Ni)/GC and Pt(Co)/GC RDEs, respectively in oxygen-saturated 0.1 M $HClO_4$ solutions, recorded for various rotation speeds at 20 mV s^{-1} in the cathodic direction. The corresponding Koutechky–Levich plots at −0.1 V vs. SCE are shown in the insets. Using the values of $D_{O2}=1.90\times10^{-5}$ cm^2 s^{-1} and $C_{O2}=1.22\times10^{-6}$ M for oxygen diffusion coefficient and concentration in an oxygen-saturated 0.1 M $HClO_4$ solution [39, 40] the number of electrons found for oxygen reduction at Pt(Ni) and Pt(Co) was n=4.1 and 4.2, respectively. These values are in accordance with the extensive literature for oxygen reduction at Pt electrodes from acid solutions (see for example [39, 40]) and indicate that at these bimetallic electrodes too, ORR follows the $4e^-$ pathway.

Figure 4a–c presents slow potential sweep voltammograms (at 5 mV s^{-1} and 500 rpm) in oxygen-saturated 0.1 M $HClO_4$ solutions at pure Pt, Pt(Ni)/GC and Pt(Co)/GC RDEs, respectively, with two different initial potential values. The first is +1.20 V vs. SCE where, according to the surface voltammetry in acid shown in Fig. 2a, a complete Pt oxide monolayer is formed (same potential as the one used for the evaluation of thicker Pt(M) electrodes in our previous studies [41–44]). The second one is +0.90 V vs. SCE corresponding, according to Fig. 2b, to a partial oxide monolayer (closer to the measured rest potential of ca. +0.80 V and to the values used in most of the voltammetric studies in the literature). One can see that although the limiting current is not significantly affected by the choice of the initial potential, there are differences in the currents recorded in the kinetic and mixed control regions. Despite the fact that for pure Pt, the foot of the voltammetric wave remains practically unchanged whether the start potential is +1.20 or +0.90 V vs. SCE, for Pt(Ni) and Pt(Co) electrodes the excursion of the potential to more positive potentials (and the resulting

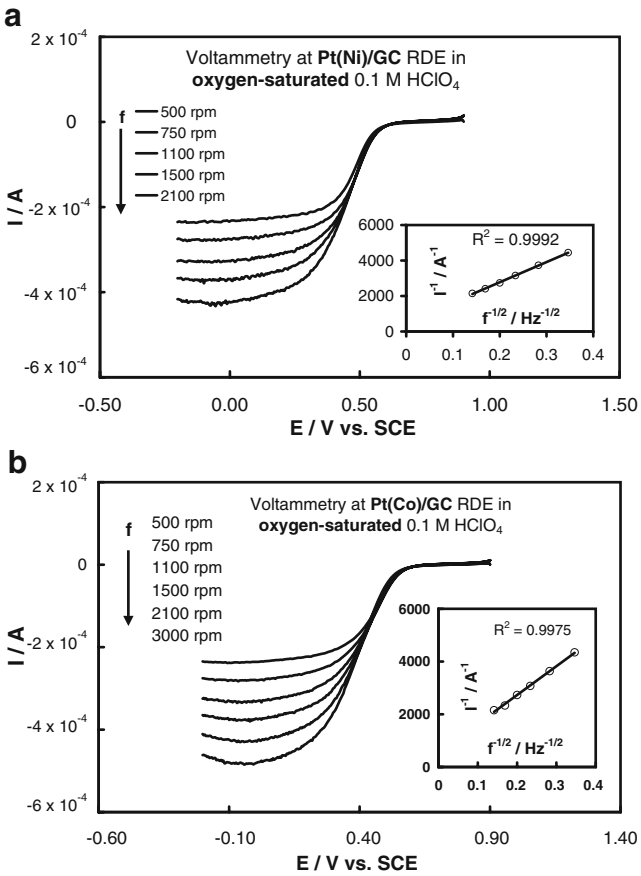

Fig. 3 Voltammograms (negative going scan at a 20 mV s^{-1} potential scan rate) of **a** a Pt(Ni)/GC RDE and **b** a Pt(Co)/GC RDE, at various rotation speeds (as indicated in the graph), in an oxygen-saturated 0.1 M $HClO_4$ solution. *Insets:* Koutecky-Levich plot at −0.1 V vs. SCE

formation of a complete Pt oxide monolayer) retards ORR until the oxides are reduced to a significant extent. The difference of the effect of the anodic limit to ORR between pure Pt and Pt(Ni), Pt(Co) electrodes can then be explained by the difference in their activity towards Pt surface oxide reduction, as discussed in the previous section.

From the voltammetric data of Fig. 4, the mass transfer-corrected $\log(i_k)_{esa}$ vs. E plots for the Pt, Pt(Ni) and Pt(Co) were constructed and are presented in Fig. 4a, b for initial potentials of +0.90 V and +1.20 vs. SCE, respectively. The mass transfer-corrected (kinetic) current density, $(i_k)_{esa}$, is given per Pt electroactive surface area (esa) and is thus representative of the inherent catalytic activity of the electrodes. Figure 5a shows that Pt(Co) and Pt(Ni) electrodes prepared by the transmetalation method, with Co and Ni compositions that are in the optimum range reported in the literature (30% and 26% atomic concentration, respectively) and which are evaluated under similar voltammetric conditions to those of relevant studies, show superior behaviour to that of pure Pt over the entire polarisation range. For example, ca. threefold and twofold enhancements of ORR

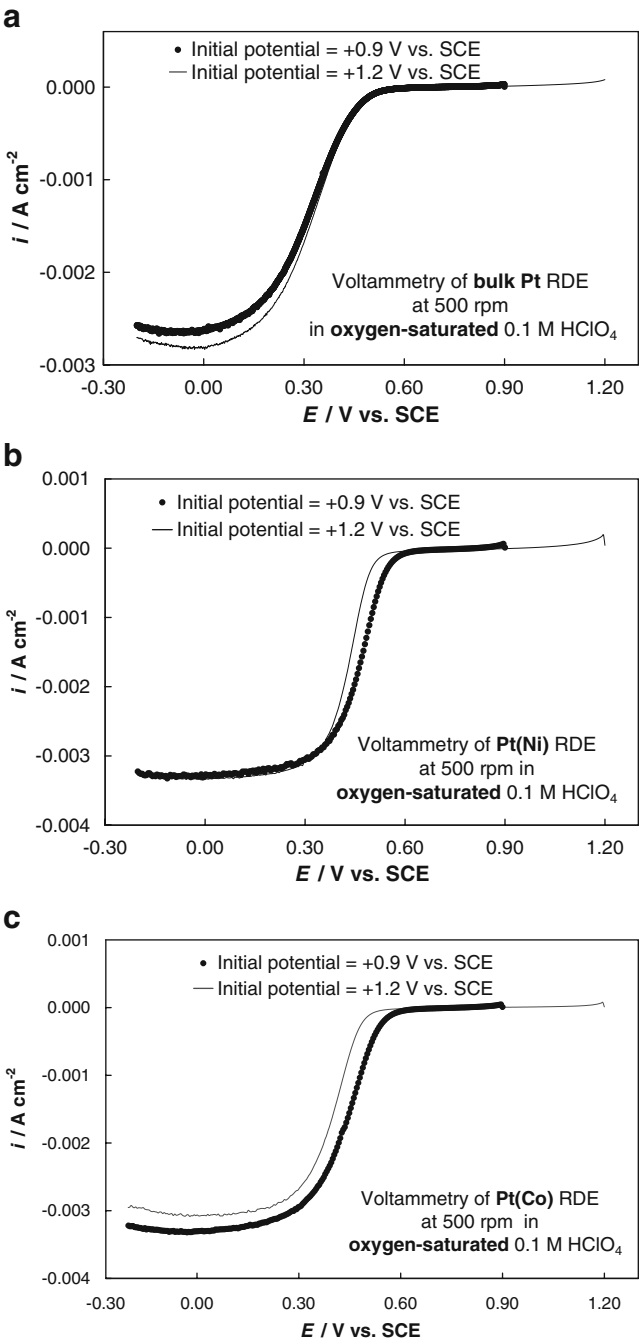

Fig. 4 Voltammograms (negative going scan at 5 mV s^{-1} potential scan rate) of **a** Pt, **b** Pt(Ni)/GC and **c** Pt(Co)/GC RDEs at 500 rpm in oxygen-saturated 0.1 M $HClO_4$ solutions, recorded from two different start potentials (+1.20 V and +0.90 V vs. SCE, as indicated in the graphs)

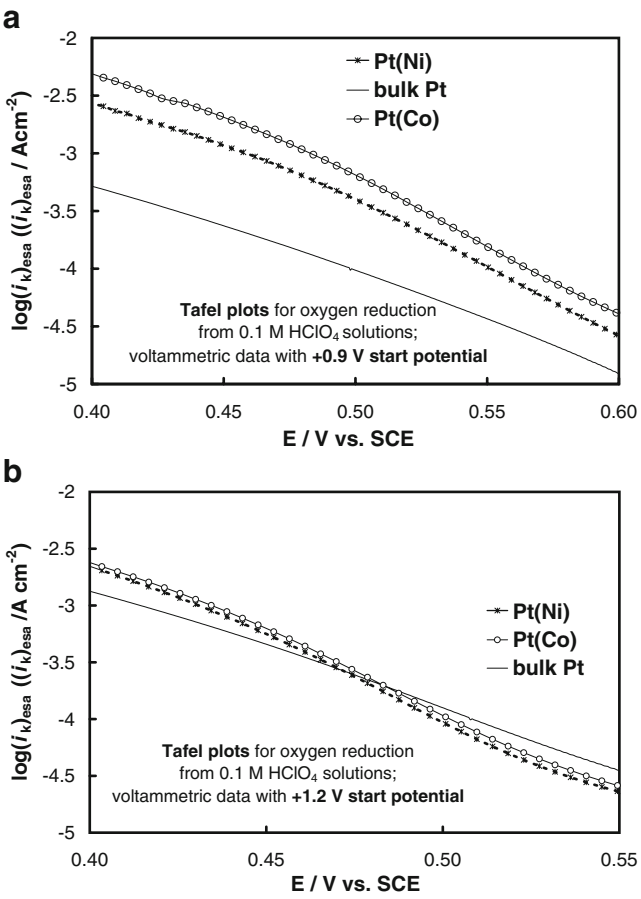

Fig. 5 Mass transfer-corrected $\log(i_k)_{esa}$ vs. E (Tafel) plots from data of Fig. 4. The start potential was +0.90 V vs. SCE (**a**) or +1.20 V vs. SCE (**b**)

catalytic activity are obtained for Pt(Co) and Pt(Ni) electrodes at +0.60 V vs. SCE (i.e. at low overpotentials, relevant to fuel cell research), within the enhancement range of many previous reports [3, 4, 13, 17–19, 21]. Figure 5b shows that when the more positive potential of +1.20 V was chosen as the initial potential for the voltammetry experiments then at low overpotentials (down to a potential of ca. 0.48 V vs. SCE) the catalytic activity of Pt(Ni) and Pt(Co) appears lower than that of pure Pt. This is because at these potentials the surface of the electrode is still covered to a large extent with Pt surface oxides that are more difficult to reduce at the Pt (Ni) and Pt(Co) electrodes (see Fig. 2a). Once these oxides start to reduce at potentials lower than ca. 0.48 V vs. SCE then the superior behaviour of the bimetallic electrodes shows up. In the case of the lower starting potential +0.90 V, a lower oxide coverage pertains even at low overpotentials (since only a part of oxide monolayer is initially present—see Fig. 2b) and its stripping is not crucial for ORR to commence at appreciable rates. The above findings highlight the importance of the choice of the initial anodic potential limit when comparing the ORR catalytic activity of Pt(M) electrodes based on slow potentiodynamic methods.

Two different interpretations of the higher ORR catalytic activity of Pt(M) electrodes (M: Fe, Co, Ni) can be found in the literature, one proposed by Ross, Markovic, Stamenkovic and co-workers [3, 4, 16–20] and one recently suggested by Watanabe and co-workers [22]. They both start from the

well-documented downward shift in Pt d-band energy centre, ε_d, in the presence of the early-transition metal underlayers; the shift has been theoretically predicted by Nørskov and co-workers (based on DFT calculations and taking into account stress and ligand effects) [48, 49] and has also been experimentally verified by direct d-band energy centre measurements with high-resolution ultraviolet photoelectron spectroscopy [18, 19] and core electron level down-shifts measured by XPS [50].

However, the first group of researchers accepts as the rate determining step of ORR at Pt surfaces that of the reductive removal of Pt–O and Pt–OH formed from fast oxygen dissociative adsorption. Based on theoretical predictions of Pt–O bond weakening at Pt(M) catalysts [47], they then attribute the high ORR activity of the latter on reduced surface oxide coverage. On the other hand, Watanabe and co-workers, based on their recent direct experimental finding of increased Pt–O coverage at Pt(Fe) electrodes, they interpret the enhancement of ORR by proposing as rate determining step that of electron uptake occurring immediately after dissociative oxygen chemisorption [22]. According to that scenario, the d-electrons of a higher lying Pt(M) Fermi level (with respect to the down-shifted core electron and d-band electron energy levels [50]) take part in increased electron back-donation to oxygen π^* orbitals. This in turn favours O–O bond scission, increases adsorbed O surface concentration and, as a result, increases the rate of electron transfer to it. Since in our results Pt surface oxides seem to be formed even when a less positive initial potential was chosen (+0.90) and these oxides were harder to reduce at Pt(M) electrodes (see Fig. 2b), then the observed ORR enhancement (Fig. 5a) can only be understood by means of Watanabe's approach: the reduction of low coverage surface oxides is not rate determining for ORR at Pt(M) electrodes but instead the, reaction is controlled by oxygen bond scission followed by electron uptake.

Conclusions

1. With appropriate control of the initial thickness of Ni and Co layers, platinized Pt(Ni) and Pt(Co) catalysts of 25–30% atomic concentration in Ni and Co could be obtained by means of the recently introduced room temperature transmetalation process.
2. The surface electrochemistry of Pt(Ni) and Pt(Co) electrodes as studied by fast cyclic voltammetry in deaerated acid solutions, indicates that these materials retard the reduction of Pt surface oxides.
3. The above-mentioned trend together with the pronounced negative effect that large quantities of surface oxides have on ORR kinetics, make the choice of the positive limit of potentiodynamic experiments crucial in accessing the catalytic activity of these bimetallic systems. When a complete Pt oxide monolayer is allowed to form at a sufficiently positive start potential, then ORR is hindered until a significant part of the oxides is reduced.
4. Pt(Ni) and Pt(Co) layers prepared by transmetalation, with a composition similar to the optimum reported in the literature and evaluated by voltammetry with a start potential close to the system's rest potential (a situation relevant to fuel cell operation), showed a moderate enhancement of ORR activity with respect to that of Pt. This enhancement was attributed to the effect of the second metal on Pt activity towards O–O bond scission followed by electron uptake.
5. The proposed alternative room temperature preparation method for improved Pt(Ni) and Pt(Co) catalysts for ORR may be of practical interest for fuel cell or sensor catalysts since it may result in lower Pt loadings and could also be used in connection with Ni, Co (and Cu) electroless deposition microfabrication techniques to prepare micro-fuel cells and sensors.

Acknowledgements ΓΓΕΤ Greece for ΠΕΝΕΔ-03ΕΔ378; IKY, Greece for a PhD Fellowship to S.P.

References

1. Mukerjee S, Srinivasan S (1993) Enhanced electrocatalysis of oxygen reduction on platinum alloys in proton exchange membrane fuel cells. J Electroanal Chem 357:201–224. doi:10.1016/0022-0728(93)80380-Z
2. Watanabe M, Tsurumi K, Mizukami T, Nakamura T, Stonehart P (1994) Activity and stability of ordered and disordered Co-Pt alloys for phosphoric acid fuel cells. J Electrochem Soc 141 (10):2659–2668. doi:10.1149/1.2059162
3. Paulus UA, Wokaun A, Scherer GG, Schmidt TJ, Stamenkovic V, Radmilovic V, Markovic NM, Ross PN (2002) Oxygen reduction on carbon-supported Pt-Ni and Pt-Co alloy catalysts. J Phys Chem B 106:4181–4191. doi:10.1021/jp0134421
4. Paulus UA, Wokaun A, Scherer GG, Schmidt TJ, Stamenkovic V, Markovic NM, Ross PN (2002) Oxygen reduction on high surface area Pt-based alloy catalysts in comparison to well defined smooth bulk alloy electrodes. Electrochim Acta 47:3787–3798. doi:10.1016/S0013-4686(02)00349-3
5. Salgado JRC, Antolini E, Gonzalez ER (2004) Preparation of Pt-Co/C electrocatalysts by reduction with borohydride in acid and alkaline media: the effect on the performance of the catalyst. J Power Sources 138:56–60. doi:10.1016/j.jpowsour.2004.06.011
6. Antolini E, Salgado JRC, Gonzalez ER (2005) Carbon supported Pt75M25 (M = Co, Ni) alloys as anode and cathode electrocatalysts for direct methanol fuel cells. J Electroanal Chem 580:145–154. doi:10.1016/j.jelechem.2005.03.023
7. Antolini E, Salgado JRC, Giz MJ, Gonzalez ER (2005) Effects of geometric and electronic factors on ORR activity of carbon supported Pt-Co electrocatalysts in PEM fuel cells. Int J Hydrogen Energy 30:1213–1220. doi:10.1016/j.ijhydene.2005.05.001

8. Antolini E, Salgado JRC, Gonzalez ER (2006) Oxygen reduction on a $Pt_{70}Ni_{30}$/C electrocatalyst prepared by the borohydride method in H_2SO_4/CH_3OH solutions. J Power Sources 155(2):161–166
9. Antolini E, Salgado JRC, Giz MJ, Gonzalez ER (2006) The stability of Pt-M (M = first row transition metal) alloy catalysts and its effect on the activity in low temperature fuel cells. A literature review and tests on a Pt-Co catalyst. J Power Sources 160:957–968. doi:10.1016/j.jpowsour.2006.03.006
10. Santos LGRA, Oliveira CHF, Moraes IR, Ticianelli EA (2006) Oxygen reduction reaction in acid medium on Pt-Ni/C prepared by a microemulsion method. J Electroanal Chem 596:141–148. doi:10.1016/j.jelechem.2006.07.033
11. Antolini E, Lopes T, Gonzalez ER (2008) An overview of platinum-based catalysts as methanol-resistant oxygen reduction materials for direct methanol fuel cells. J Alloy Comp 461:253–262. doi:10.1016/j.jallcom.2007.06.077
12. Baglio V, Stassi A, DiBlasi A, D'Urso C, Antonucci V, Arico AS (2007) Investigation of bimetallic Pt-M/C as DMFC cathode catalysts. Electrochim Acta 53:1361–1365. doi:10.1016/j.electacta.2007.04.099
13. Yano H, Song JM, Uchida H, Watanabe M (2008) Temperature dependence of oxygen reduction activity at carbon-supported Pt_xCo (X = 1, 2, and 3) alloy catalysts prepared by the nanocapsule method. J Phys Chem C 112:8372–8380. doi:10.1021/jp712025q
14. Toda T, Igarashi H, Uchida H, Watanabe M (1999) Enhancement of the electroreduction of oxygen on Pt alloys with Fe, Ni, and Co. J Electrochem Soc 146(10):3750–3756. doi:10.1149/1.1392544
15. Toda T, Igarashi H, Uchida H, Watanabe M (1999) Enhancement of the electrocatalytic O_2 reduction on Pt-Fe alloys. J Electroanal Chem 460:258–262. doi:10.1016/S0022-0728(98)00361-1
16. Stamenkovic VR, Schmidt TJ, Ross PN, Markovic NM (2002) Surface composition effects in electrocatalysis: kinetics of oxygen reduction on well-defined Pt_3Ni and Pt_3Co alloy surfaces. J Phys Chem B 106:11970–11979. doi:10.1021/jp021182h
17. Stamenkovic VR, Mun BS, Mayrhofer KJJ, Ross PN, Markovic NM, Rossmeil J, Greeley J, Nørskov JK (2006) Changing the activity of electrocatalysts for oxygen reduction by tuning the surface electronic structure. Angew Chem Int Ed 45:2897–2901. doi:10.1002/anie.200504386
18. Stamenkovic VR, Mun BS, Mayrhofer KJJ, Ross PN, Markovic NM (2006) Effect of surface composition on electronic structure, stability, and electrocatalytic properties of Pt-transition metal alloys: Pt-skin versus Pt-skeleton surfaces. J Am Chem Soc 128 (7):8813–8819. doi:10.1021/ja0600476
19. Stamenkovic VR, Mun BS, Arenz M, Mayrhofer KJJ, Lucas CA, Wang G, Ross PN, Markovic NM (2007) Trends in electrocatalysis on extended and nanoscale Pt-bimetallic alloy surfaces. Nat Mater 6:241–247. doi:10.1038/nmat1840
20. Stamenkovic VR, Fowler B, Mun BS, Wang G, Ross PN, Lucas CA, Markovic NM (2007) Improved oxygen reduction activity on $Pt_3Ni(111)$ via increased surface site availability. Science 315:493–497. doi:10.1126/science.1135941
21. Bonakdarpour A, Lake K, Stevens K, Dahn JR (2008) Oxygen reduction activity of magnetron-sputtered $Pt_{1-x}Co_x$($0 \le x \le 0.5$) films. J Electrochem Soc 155(2):B108–B118. doi:10.1149/1.2806166
22. Wakisaka M, Suzuki H, Mitsui S, Uchida H, Watanabe M (2008) Increased oxygen coverage at Pt-Fe alloy cathode for the enhanced oxygen reduction reaction studied by EC-XPS. J Phys Chem C 112:2750–2755. doi:10.1021/jp0766499
23. Mukerjee S, Srinivasan S, Soriaga MP (1995) Role of structural and electronic properties of Pt and Pt alloys on electrocatalysis of oxygen reduction. J Electrochem Soc 142(5):1409–1422. doi:10.1149/1.2048590
24. Min M, Cho J, Cho K, Kim H (2000) Particle size and alloying effects of Pt-based alloy catalysts for fuel cell applications. Electrochim Acta 45:4211–4217. doi:10.1016/S0013-4686(00)00553-3
25. Yuan W, Scott K, Cheng H (2006) Fabrication and evaluation of Pt-Fe alloys as methanol tolerant cathode materials for direct methanol fuel cells. J Power Sources 163:323–329. doi:10.1016/j.jpowsour.2006.09.005
26. Baglio V, Arico AS, Stassi A, D'Urso C, DiBlasi A, Luna AMC, Antonucci V (2006) Investigation of Pt-Fe catalysts for oxygen reduction in low temperature direct methanol fuel cells. J Power Sources 159(2):900–904. doi:10.1016/j.jpowsour.2005.12.088
27. Antolini E (2003) Formation of carbon-supported PtM alloys for low temperature fuel cells: a review. Mater Chem Phys 78:563–573. doi:10.1016/S0254-0584(02)00389-9
28. Antolini E, Salgado JRC, DaSilva RM, Gonzalez ER (2007) Preparation of carbon supported binary Pt-M alloy catalysts (M = first row transition metals) by low/medium temperature methods. Mater Chem Phys 101:395–403. doi:10.1016/j.matchemphys.2006.07.004
29. Ruban AV, Skriver HL, Nørskov JK (1999) Surface segregation energies in transition-metal alloys. Phys Rev B: Condens Matter 29(24):15990–16000. doi:10.1103/PhysRevB.59.15990
30. Brankovic SR, Wang JX, Adzic RR (2001) Metal monolayer deposition by replacement of metal adlayers on electrode surfaces. Surf Sci 474:L173–L179. doi:10.1016/S0039-6028(00)01103-1
31. Brankovic SR, Wang JX, Zhu Y, Sabatini R, McBreen J, Adzic RR (2002) Electrosorption and catalytic properties of bare and Pt modified single crystal and nanostructured Ru surfaces. J Electroanal Chem 524:231–241. doi:10.1016/S0022-0728(02)00667-8
32. Sasaki K, Mo Y, Wang JX, Balasubramanian M, Uribe F, McBreen J, Adzic RR (2003) Pt submonolayers on metal nanoparticles—novel electrocatalysts for H_2 oxidation and O_2 reduction. Electrochim Acta 48:3841–3849. doi:10.1016/S0013-4686(03)00518-8
33. Zhang J, Mo Y, Vukmirovic MB, Klie K, Sasaki K, Adzic RR (2004) Platinum monolayer electrocatalysts for O_2 reduction: Pt monolayer on Pd(111) and on carbon-supported Pd nanoparticles. J Phys Chem B 108:10955–10964. doi:10.1021/jp0379953
34. Zhang J, Lima FHB, Shao MH, Sasaki K, Wang JX, Adzic RR (2005) Platinum monolayer on nonnoble metal-noble metal core-shell nanoparticle electrocatalysts for O_2 reduction. J Phys Chem B 109:22701–22704. doi:10.1021/jp055634c
35. Zhang J, Vukmirovic MB, Sasaki K, Nilekar AU, Mavrikakis M, Adzic RR (2005) Mixed-metal Pt monolayer electrocatalysts for enhanced oxygen reduction kinetics. J Am Chem Soc 127:12480–12481. doi:10.1021/ja053695i
36. Shao MH, Huang T, Liu P, Zhang J, Sasaki K, Vukmirovic MB, Adzic RR (2006) Palladium monolayer and palladium alloy electrocatalysts for oxygen reduction. Langmuir 22:10409–10415. doi:10.1021/la0610553
37. Vukmirovic MB, Zhang J, Sasaki K, Nilekar AU, Uribe F, Mavrikakis M, Adzic RR (2007) Platinum monolayer electrocatalysts for oxygen reduction. Electrochim Acta 52:2257–2263. doi:10.1016/j.electacta.2006.05.062
38. Lima FHB, Zhang J, Sao MH, Sasaki K, Vukmirovic MB, Ticianelli EA, Adzic RR (2007) Catalytic activity—d-band center correlation for the O_2 reduction reaction on platinum in alkaline solutions. J Phys Chem C 111:404–410. doi:10.1021/jp065181r
39. Van Brussel M, Kokkinidis G, Vandendael I, Buess-Herman C (2002) High performance gold-supported platinum electrocatalyst for oxygen reduction. Electrochem Commun 4(10):808–813. doi:10.1016/S1388-2481(02)00437-X
40. Van Brussel M, Kokkinidis G, Hubin A, Buess-Herman C (2003) Oxygen reduction at platinum modified gold electrodes. Electrochim Acta 48:3909–3919. doi:10.1016/S0013-4686(03)00529-2
41. Papadimitriou S, Tegou A, Pavlidou E, Kokkinidis G, Sotiropoulos S (2007) Methanol oxidation at platinized lead coatings prepared by a two-step electrodeposition-electroless deposition process on glassy carbon and platinum substrates. Electrochim Acta 52:6254–6260. doi:10.1016/j.electacta.2007.04.020

42. Tegou A, Papadimitriou S, Pavlidou E, Kokkinidis G, Sotiropoulos S (2007) Oxygen reduction at platinum- and gold-coated copper deposits on glassy carbon substrates. J Electroanal Chem 608:67–77. doi:10.1016/j.jelechem.2007.05.008
43. Papadimitriou S, Tegou A, Pavlidou E, Kokkinidis G, Sotiropoulos S (2008) Preparation and characterisation of platinum- and gold-coated copper, iron, cobalt and nickel deposits on glassy carbon substrates. Electrochim Acta 53:6559–6567. doi:10.1016/j.electacta.2008.04.015
44. Tegou PS, Armyanov S, Valova E, Kokkinidis G, Sotiropoulos S (2008) Oxygen reduction at platinum- and gold-coated iron, cobalt, nickel and lead deposits on glassy carbon substrates. J Electroanal Chem 623:187–196. doi:10.1016/j.jelechem.2008.07.012
45. Callister WD Jr (1997) Materials science and engineering: an introduction, 4th edn. Wiley, New York
46. Shimazu K, Weisshaar D, Kuwana T (1987) Electrochemical dispersion of Pt microparticles on glassy carbon electrodes. J Electroanal Chem 223:223–234. doi:10.1016/0022-0728(87)85262-2
47. Nørskov JK, Rossmeisi J, Logadottir A, Lindqvist L, Kitchin JR, Bligaard T, Jónsson H (2004) Origin of the overpotential for oxygen reduction at a fuel-cell cathode. J Phys Chem B 108:17886–17892. doi:10.1021/jp047349j
48. Ruban A, Hammer B, Stoltze P, Skriver HL, Nørskov JK (1997) Surface electronic structure and reactivity of transition and noble metals. J Mol Catal A: Chem 115:421–429. doi:10.1016/S1381-1169(96)00348-2
49. Kitchin JR, Nørskov JK, Barteau MA, Chen JGJ (2004) Modification of the surface electronic and chemical properties of Pt(111) by subsurface 3d transition metals. J Chem Phys 120 (21):10240–10246. doi:10.1063/1.1737365
50. Wakisaka M, Mitsui S, Hirose Y, Kawashima K, Uchida H, Watanabe M (2006) Electronic structures of Pt-Co and Pt-Ru alloys for CO-tolerant anode catalysts in polymer electrolyte fuel cells studied by EC-XPS. J Phys Chem B 110:23489–23496. doi:10.1021/jp0653510